NATURAL NANOFLUID CONVECTION IN RECTANGULAR POROUS DOMAINS

by

Hamza SAYYOU*, Jabrane BELABID, and Karam ALLALI

Laboratory of Mathematics, Computer Science and Applications,
Faculty of Sciences and Technologies, University Hassan II of Casablanca, Mohammedia, Morocco

Original scientific paper
https://doi.org/10.2298/TSCI230405178S

In this paper, the free convective flow and heat transfer in a porous rectangular enclosures filled with Cu-water nanofluid is studied and analyzed. The cavity side-walls are exposed to a constant heat flux and the horizontal walls are assumed to be adiabatic. The governing equations describing the problem are solved using a finite difference method. The main parameters of our problem are: aspect ratio, volume fraction of nanoparticles, types of media, porosity of the medium, and Rayleigh number. The results indicate that an increase in aspect ratio from 0.1 to 0.7 leads to a significant increase of Nusselt number, which then reaches a maximum value. However, the heat transfer rate progressively decreases for aspect ratios greater than 0.7. Moreover, the addition of Cu-nanoparticles weakens the heat transfer. As a result, when the porous medium has low thermal conductivity, the solid matrix porosity becomes particularly more effective in improving heat transfer. Also, a correlation was established between the average Nusselt number and the influencing parameters. Results show that the governing parameters impact the flow regime.

Key words*: natural convection, porous medium, aspect ratio, rectangular cavity, nanofluid*

Introduction

Natural convection is a fundamental mode of heat transfer that occurs when a fluid is heated and moved, displacing cooler fluid in the process. The phenomenon has been studied extensively due to its practical applications in various fields, including building design, electronics cooling, renewable energy systems, underground transmission lines, and food processing [1, 2]. In addition, there are many types of convection and several investigations have been examined the heat and mass transfer. Chamkha and Al-Naser [3] investigated thermosolutal convection in a porous enclosure. Their results shows that heat and mass transfer as well as flow circulation inside the cavity are both decreased by lowering the Darcy number and raising the inclination angle. Double-diffusive convection in a rectangular cavity submitted to magnetic field is studied in another work of Chamkha and Al-Naser [4]. Chamkha *et al*. [5] analyzed mixed convection from a heated square solid cylinder at the center of a vented cavity. The paper of Khanafer and Chamkha [6] studied hydro-magnetic natural convection in tilted porous square

*Corresponding author, e-mail: hamzasayyou@gmail.com

cavity with heat generation. It was found that the magnetic field, inclination angle and Darcy number greatly affected heat transfer mechanisms and flow properties inside the inclined enclosure.

Recent studies have focused on the application of natural convection in micro-fluidics, such as micro-channels, micro-reactors, and micro-heat exchangers. For instance, the study by Jung and Park [7] investigated the heat transfer enhancement of natural convection in a micro-channel heat sink using Al_2O_3-water nanofluid. Another recent study by Sharifpur *et al.* [8] investigated the natural convection heat transfer performance in a cavity filled with TiO_2-water nanofluid. They found that the heat transfer rate attain the maximum for 0.05% nanoparticle volume fraction. Anwar *et al.* [9] performed a numerical study on convective flow in heat sinks of a mini-channel saturated with CuO-water nanofluid for microprocessor cooling.

Nanofluids are a type of fluid that contain suspended nanoparticles, typically less than 100 nm in size, in a base fluid. The addition of nanoparticles to the base fluid can significantly affect its thermal conductivity and convective heat transfer coefficient, leading to improved heat transfer rates. Nanofluids can be synthesized using various types of nanoparticles, such as metal oxides, carbides, nitrides, and carbon-based materials, and base fluids, such as water, ethylene glycol, and oil, Keblinski *et al.* [10]. Nanofluids have been studied in various geometries and configurations Asmadi *et al.* [11], Rahimi *et al.* [12], Sadeghi *et al.* [13], Izadi *et al.* [14], and Hashemi-Tilehnoee *et al.* [15], explored their potential applications in heat exchangers, solar collectors, and cooling systems, among others. For example, the study by Xu *et al.* [16] investigated the thermal performance of a flat plat solar collector filled with Al_2O_3-water nanofluid and found that the collector's efficiency is impacted by the nanoparticles. Another study by Alklaibi *et al.* [17] examined the heat transfer characteristics of a plate heat exchanger using MWCNT + Fe_3O_4-water hybrid nanofluid. A study was conducted by Yao *et al.* [18] using the lattice Boltzmann method to investigate free convection heat transfer flow in a porous-partial cavity with the application of different kinds of nanoparticles (Al_2O_3, Cu, and SiO_2). The study of natural convection of a Cu-nanofluid subjected to a magnetic field using the control volume finite element method was examined by Dogonchi *et al.* [19]. They reported that convective flow strength increases with increasing Rayleigh number and decreases with increasing Hartmann number and wavy contraction ratio. The same numerical method was applied by Chamkha *et al.* [20] to study thermal radiation and nanoparticles shape factor impacts on nanoliquid MHD natural convection within a cavity. A numerical study was conducted by Alsabery *et al.* [21] to investigate mixed convection Al_2O_3 nanofluid in a square cavity with double lid-driven including a solid body. It was observed that the heat transfer rate decreased as the block's size and Richardson number increased.

One of the key parameters affecting natural convection is the aspect ratio of the cavity, which is the ratio of its length to its width. The aspect ratio can have a significant impact on the heat transfer characteristics of the system, affecting the flow patterns, temperature distribution, and heat transfer rate. Understanding the effect of aspect ratio is important for designing and optimizing heat transfer systems in various applications. Recent studies have explored the effect of aspect ratio on natural convection in various geometries, such as annular cavities Belabid *et al.* [22] and rectangular cavities Oztop and Abu-Nada [23]. These studies highlight the importance of understanding the impact of aspect ratio on natural convection for various geometries and applications. Another recent study by Redouane *et al.* [24] investigated the natural convection in a porous triangular corrugated enclosure with a rotate centered cylindrical cavity filled with Ag-MgO-water hybrid nanofluid.

This article examines how the aspect ratio and other parameters affect natural convection and flow pattern in a rectangular cavity filled with a Cu-water nanofluid. Our aim is to analyze the heat transfer characteristics of the physical system and determine how the aspect ratio impacts the convective heat transfer rate. In this analysis we adopt the mathematical model of Tiwari and Das [25], and it builds upon the existing literature on free convection in enclosures filled with nanofluids, it sheds light on the complex interplay between the geometry of the cavity and the properties of the nanofluid. The amount of studies conducted on the influence of aspect ratio on natural convection in cavities containing nanofluids is constrained, and our study fills this gap in the literature. The results of our study could have practical implications for the design and optimization of heat transfer systems in various applications, including electronics cooling, power generation and renewable energy systems. The novelty of this paper lies in examining the heat transfer and the flow regime with the presence of Cu-nanoparticles for different values of aspect ratio not treated before for a rectangular enclosure.

Mathematical formulation of the problem

The geometrical configuration and the chosen boundary conditions of the present study is illustrated in fig. 1. Considering a 2-D saturated porous cavity of the height, H, and the width, L, such that the aspect ratio $Ar = H/L$ containing a Cu-water nanofluid. The enclosure heated constantly from the left side, T_{hot}, and the right one is cooled, T_{cold}, while the top and bottom walls are thermally insulated, $\partial\tilde{T}/\partial y = 0$. We admit that the porous medium in thermal equilibrium. The mixture is incompressible, Newtonian and flow pattern is laminar.

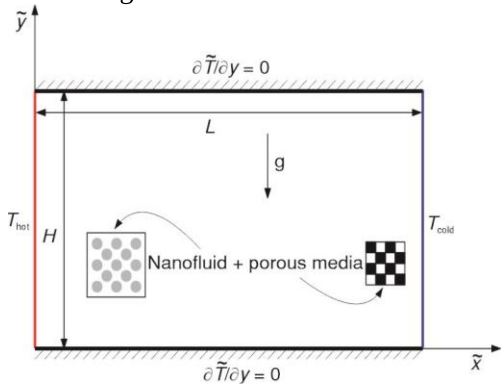

Figure 1. Sketch of the physical problem

The effective thermal physical parameters

All the thermophysical properties are supposed to be unchanged, except for density in the buoyancy term, depending on the Darcy-Boussinesq model. The porous matrix composed of the aluminium foam or the glass balls is homogeneous and isotropic. The thermal physical parameters of water, solid matrix and nano-size particles are cited in tab. 1. The following thermal physical expressions have been noticed in Abu-Nada and Oztop [26] and Haddad *et al.* [27].

Table 1. The base fluid, the nanoparticles, and the solid structure thermophysical properties [28]

Physical properties	Clear fluid (water)	Cu	Aluminium foam	Glass balls
C_p [Jkg^{-1}K^{-1}]	4179	385	897	840
ρ [kgm^{-3}]	997.1	8933	2700	2700
k [Wm^{-1}K^{-1}]	0.613	400	205	1.05
$\beta\times10^{-5}$ [K^{-1}]	21	1.67	2.22	0.9

The heat capacitance of the nanofluid can be determined by:

$$(\rho C_p)_{\text{nf}} = (1-\varphi)(\rho C_p)_{\text{f}} + \varphi(\rho C_p)_{\text{p}} \tag{1}$$

The thermal conductivity of the nanofluid represented by:

$$k_{\mathrm{nf}} = k_{\mathrm{f}} \left[\frac{k_{\mathrm{p}} + 2k_{\mathrm{f}} - 2\varphi\left(k_{\mathrm{f}} - k_{\mathrm{p}}\right)}{k_{\mathrm{p}} + 2k_{\mathrm{f}} + \varphi\left(k_{\mathrm{f}} - k_{\mathrm{p}}\right)} \right] \tag{2}$$

The nanofluid viscosity approximated in function of base fluid viscosity expressed as:

$$\mu_{\mathrm{nf}} = \frac{\mu_{\mathrm{f}}}{(1-\varphi)^{2.5}} \tag{3}$$

The buoyancy coefficient of the nanofluid is:

$$(\rho\beta)_{\mathrm{nf}} = (1-\varphi)(\rho\beta)_{\mathrm{f}} + \varphi(\rho\beta)_{\mathrm{p}} \tag{4}$$

The heat capacitance of the medium is:

$$\left(\rho C_p\right)_{\mathrm{m}} = \varepsilon\left(\rho C_p\right)_{\mathrm{f}} + (1-\varepsilon)\left(\rho C_p\right)_{\mathrm{s}} \tag{5}$$

More physical properties are shown as:

$$k_{\mathrm{m}} = \varepsilon k_{\mathrm{f}} + (1-\varepsilon)k_{\mathrm{s}} \tag{6}$$

The thermal conductivity of nanofluid saturated porous medium is:

$$\begin{aligned} k_{\mathrm{mnf}} &= \varepsilon k_{\mathrm{nf}} + (1-\varepsilon)k_{\mathrm{s}} \\ &= \varepsilon k_{\mathrm{nf}} + k_{\mathrm{m}} - \varepsilon k_{\mathrm{f}} \end{aligned} \tag{7}$$

Governing equations

Taking into consideration the above assumptions, the dimensional fluid-flow and heat transfer equations are expressed:

– Continuity equation

$$\nabla \cdot \tilde{V} = 0 \tag{8}$$

– Darcy law equation

$$-\frac{\mu_{\mathrm{nf}}}{K}\tilde{V} = \nabla\tilde{P} + (\rho\beta)_{\mathrm{nf}}\,\mathbf{g}\,(\tilde{T} - T_{\mathrm{cold}}) \tag{9}$$

– Energy equation

$$(\tilde{V}\cdot\nabla)\tilde{T} = \frac{k_{\mathrm{mnf}}}{(\rho C_p)_{\mathrm{nf}}}\nabla^2\tilde{T} \tag{10}$$

Furthermore, we can introduce the following non-dimensional parameters as:

$$(x, y) = \left(\frac{\tilde{x}}{L}, \frac{\tilde{y}}{L}\right),\ u = \frac{\tilde{u}\,(\rho C_p)_{\mathrm{nf}}}{k_{\mathrm{mnf}}},\ v = \frac{\tilde{v}\,(\rho C_p)_{\mathrm{nf}}}{k_{\mathrm{mnf}}},\ \theta = \frac{\tilde{T} - T_{\mathrm{cold}}}{T_{\mathrm{hot}} - T_{\mathrm{cold}}}$$

The following non-dimensional velocity components defined such that:

$$V = (u, v) = \left(\frac{\partial\psi}{\partial y}, -\frac{\partial\psi}{\partial x}\right)$$

Moreover, the dimensionless stream-function temperature formulation obtained is:

$$\frac{\partial^2\psi}{\partial x^2}+\frac{\partial^2\psi}{\partial y^2}=-\mathrm{Ra}\frac{k_\mathrm{m}}{k_\mathrm{mnf}}\frac{(\rho C_p)_\mathrm{nf}}{(\rho C_p)_\mathrm{f}}\frac{\mu_\mathrm{f}}{\mu_\mathrm{nf}}\frac{(\rho\beta)_\mathrm{nf}}{(\rho\beta)_\mathrm{f}}\frac{\partial\theta}{\partial x} \tag{11}$$

$$\frac{\partial\psi}{\partial y}\frac{\partial\theta}{\partial x}-\frac{\partial\psi}{\partial y}\frac{\partial\theta}{\partial x}=\frac{\partial^2\theta}{\partial x^2}+\frac{\partial^2\theta}{\partial y^2} \tag{12}$$

where the Rayleigh number of the medium is:

$$\mathrm{Ra}=\frac{K\mathrm{g}H(\rho\beta)_\mathrm{f}(\rho C_p)_\mathrm{f}(T_\mathrm{hot}-T_\mathrm{cold})}{k_\mathrm{m}\mu_\mathrm{f}}$$

Besides, the non-dimensional boundary conditions associated to the dimensionless eqs. (11) and (12) are:

$$\begin{aligned}&\text{for}\quad x=0: \quad \theta=1 \quad\text{and}\quad \psi=0\\&\text{for}\quad x=1: \quad \theta=0 \quad\text{and}\quad \psi=0\\&\text{for}\quad y=0, Ar: \quad \partial\theta/\partial y=0 \quad\text{and}\quad \psi=0\end{aligned} \tag{13}$$

For a better analysis of the phenomenon, we had to measure the heat transfer ratio at the hot side using the local and average Nusselt number:

$$\mathrm{Nu}=\left(-\frac{k_\mathrm{mnf}}{k_\mathrm{m}}\right)\frac{\partial\theta}{\partial x}\bigg|_{x=0},\ \mathrm{Nu}_\mathrm{avg}=\frac{1}{Ar}\int_0^{Ar}\mathrm{Nu}\,\mathrm{d}y \tag{14}$$

Numerical methods

In this numerical study, a finite difference second order and accuracy scheme applied to solve the coupled eqs. (11) and (12) governed this problem corresponding to the boundary conditions (13). Those equations are descended from the equations of mass (8), momentum (9), and energy (10). The discretized algebraic linear system was calculated iteratively using successive under-relaxation techniques. The convergence criterion for all dependent variables is less than 10^{-8}. As shown in tab. 2, the code validations was carried out by comparing the mean Nusselt number, Nu_avg, with some notable investigations.

Table 2. Comparison of the average Nusselt number with the previous works for $\varphi = 0$ (clear fluid) and square form $Ar = 1$

References	Rayleigh number		
	10	100	1000
[29]	–	4.2	15.8
[30]	–	3.141	13.448
[31]	–	3.118	13.637
[32]	1.079	3.16	14.06
[33]	–	–	13.914
[28]	1.079	3.115	13.667
[34]	–	3.101	13.280
[35]	–	3.146	13.576
This study	1.070	3.120	13.893

In addition, as depicted in tab. 3 we were compare our calculation results with the presented work of Ghalambaz *et al.* [36].

Table 3. Comparison of the average Nusselt numbers with $\varphi = 0$, $\varepsilon = 0.9$ and $k_s = 2k_f$

	Ra = 1000	$Ar = 0.1$	$Ar = 10$
Our results	Nu_{avg}	1.723	5.146
[36]		1.667	5.083

Besides, a grid independency test was performed see tab. 4, it permits us to select 250 × 250 mesh as the suitable for our coming analysis which is ensure a grid-independent solution.

Table 4. The Nu_{avg} variation for different grid size with Ra = 1000, $Ar = 10$, $\varphi = 0.05$, and $\varepsilon = 0.8$ (aluminium foam)

Grid size (i × j)	Nu_{avg}	$\Delta = \dfrac{\left\lvert Nu_{avg_{(i\times j)}} - Nu_{avg_{(250\times 250)}} \right\rvert}{Nu_{avg_{(i\times j)}}} 100\%$
100 × 100	328.598	2.454%
150 × 150	323.893	1.037%
200 × 200	321.717	0.368%
250 × 250	320.532	–
300 × 300	319.818	0.223%
350 × 350	319.359	0.367%
400 × 400	319.049	0.464%

Results and discussion

In this numerical investigation, the results are obtained for this following ranges of the governing parameters; the aspect ratio of the enclosure, $Ar = 0.1$-10, the nanoparticles volume fraction, $\varphi = 0$-0.05, the porosity of the matrix, $\varepsilon = 0.3$-0.8, the Rayleigh number, Ra = 10-1000. At last, we consider two types of solid matrix the glass balls and the aluminium foam.

Figure 2 shows the variation of the Nusselt average number with the aspect ratio for a base fluid. It is observed that the heat transfer boosts significantly for the range $0.1 \leq Ar \leq 0.7$. However, the Nusselt number tends to decrease gradually for $0.7 \leq Ar \leq 10$. It can also be seen that the Rayleigh number is a good parameter for managing the heat and flow improvement within the enclosure. Apparently, in fig. 3 the porous matrix composition is negligible for a

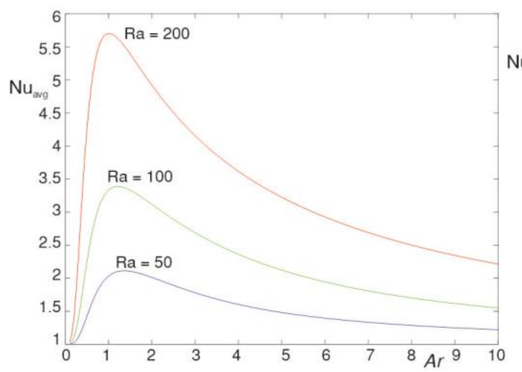

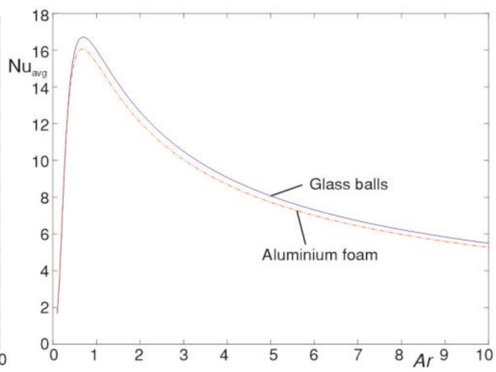

Figure 2. The Nu_{avg} *vs.* Ar for a different values of Rayleigh number with $\varphi = 0$ Figure 3. The Nu_{avg} *vs.* Ar for different values of porosity taking $\varphi = 0.05$ and Ra = 1000 for the glass balls solid matrix

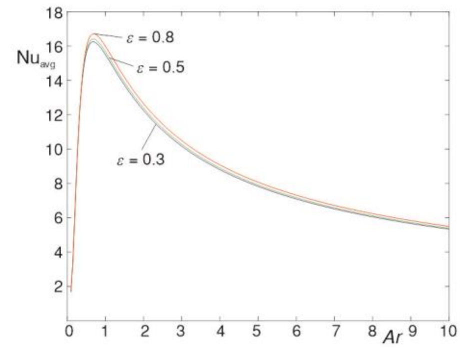

Figure 4. The Nu_{avg} *vs.* *Ar* for and for the two types of porous matrices

small aspect ratios. In contrast, it becomes more efficient with *Ar* up to 0.4. Also, fig. 4 illustrates that for a given volume fraction, incrementing the porosity affect the heat transfer as previous for high values of aspect ratio, it is more pronounced with glass balls than aluminium foam solid matrices.

Furthermore, in fig. 5 we can see the variation of the temperature rate along the left wall Nu_{avg} *vs*. nanoparticles volume fraction, φ, using two types of porous media and three values of porosity. The results reveals that in case of the glass balls and for small *Ar* less than 0.35 the average Nusselt number raise with increasing of ε and it becomes the opposite behavior for *Ar* greater than the reflection value 0.35 and it is more remarkable in case of *Ar* = 0.5. Besides, for the aluminium foam, changes in porosity values do not affect the Nu_{avg}. Moreover, adding more nanoparticles attenuate the heat transfer inside the cavity, in fact, the fluid with presence of the nanoparticles become more viscous. Essentially, for a high Rayleigh numbers the strength of the heat transfer is impacted by the effective viscosity and the thermal conductivity of the porous media.

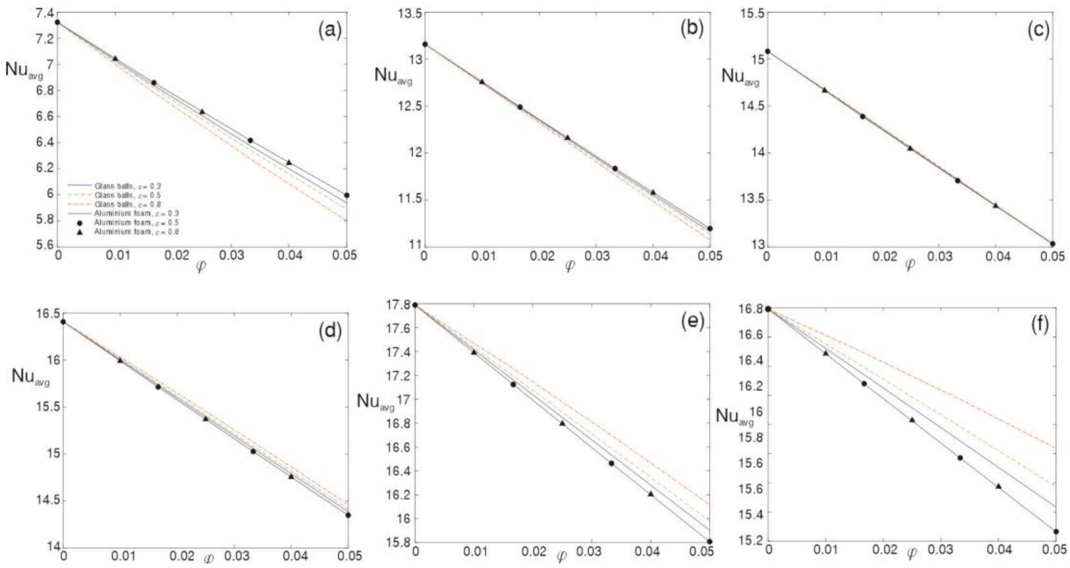

Figure 5. The influence of volume fraction φ on Nu_{avg} for Ra = 1000 for different values of porosity and porous medium; (a) *Ar* = 0.2, (b) *Ar* = 0.3, (c) *Ar* = 0.35, (d) *Ar* = 0.4, (e) *Ar* = 0.5, (f) *Ar* = 1

Figure 6 the results are presented in form of streamlines and isotherms for $0.1 \leq Ar \leq 1$. It is noticed that in case of very small aspect ratio *Ar* = 0.1 (a wide cavity) and for a high values of Rayleigh number the Nusselt average is small. The distribution of temperature is almost linear and we have a small circulation zone, it can be concluded that the heat is transferred by conduction throughout the enclosure. In addition, it's not worth mentioning that the porous structure has no important effect for the lowest aspect ratio. For the values of *Ar* between 0.2

and 0.7 the flow pattern is formed by a two flow circulations cells inside the cavity, it is owing to the temperature difference between the two walls, this formation remain visible with less thermal conductivity (glass balls). It is also observed that the two cells regime still developed for relatively low thermal conductivity values.

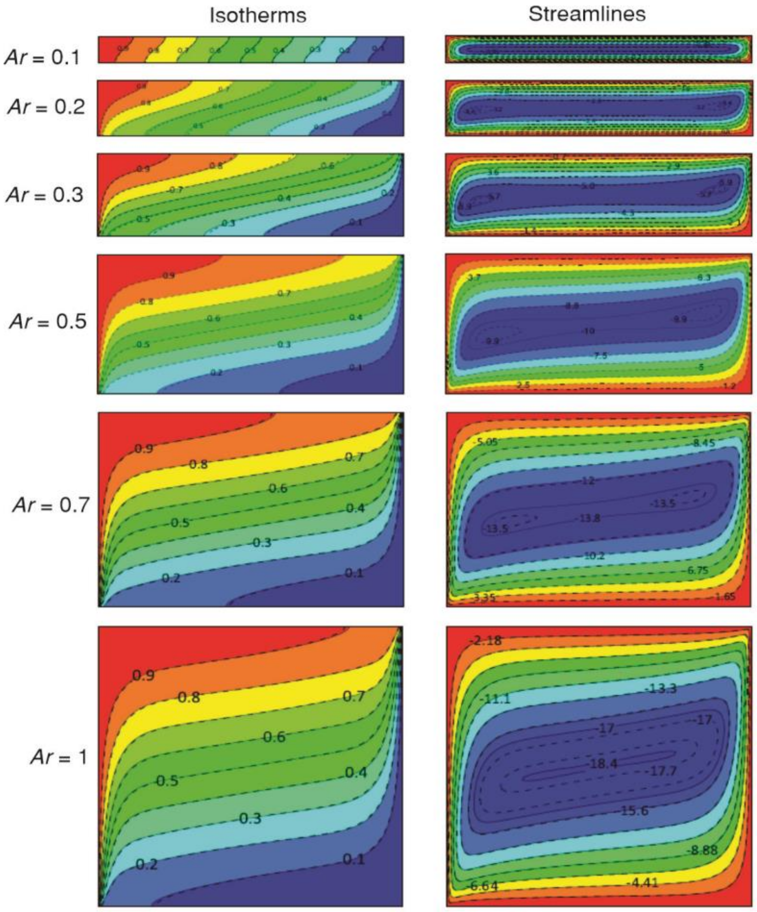

Figure 6. Isotherms and streamlines for *Ar* = 0.1-1 with glass balls (dashed lines) and aluminium foam (solid lines) solid matrices at Ra = 1000, φ = 0.05, and ε = 0.5

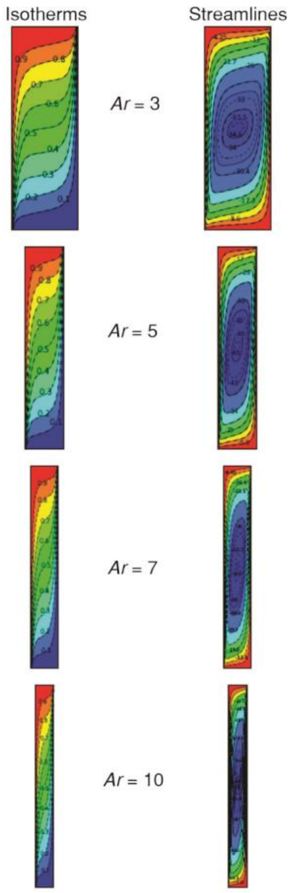

Figure 7. Isotherms and streamlines for *Ar* = 3-10 with glass balls (dashed lines) and aluminium foam (solid lines) solid matrices at Ra = 1000, φ = 0.05, and ε = 0.5

The obtained results in fig. 7 are constituted by the contours of the temperature distribution and the flow pattern ranged the aspect ratio between 3 and 10. As much we increase *Ar* (a tall cavity) the flow stream is strengthened. Besides, near the top (*i.e.* bottom) insulated boundary a hot (*i.e.* cold) layer is formed, and the middle is thermally stratified. Eventually, the heat enhancement decreases slowly by incrementing *Ar* above 1.

The resulting streamlines as shown in figs. 6 and 7 prove that the presence of the porous aluminium foam matrix strengthens the flow for all aspect ratio values and a fixed value for the volume fraction of nanoparticles and porosity. Finally, as illustrated in tab. 5 we determined the relationship between the average Nusselt number and the variables that impacted the results of the current investigation. The relationship is described in tab. 5.

Table 5. Average Nusselt number correlations for Ra = 50-200, φ = 0-0.05, and ε = 0.5

Ar	Porous matrix	Correlation	R^2
0.5	Aluminium foam	$1.383 \times 10^{-2} \times \mathrm{Ra} - 4.64085 \times \varphi + 8.74723 \times 10^{-1}$	0.98758
	Glass balls	$1.3743 \times 10^{-2} \times \mathrm{Ra} - 3.88665 \times \varphi + 8.83023 \times 10^{-1}$	0.98658
1	Aluminium foam	$2.0103 \times 10^{-2} \times \mathrm{Ra} - 5.79577 \times \varphi + 1.05230$	0.99668
	Glass balls	$2.0173 \times 10^{-2} \times \mathrm{Ra} - 4.64816 \times \varphi + 1.04524$	0.99697
5	Aluminium foam	$1.0193 \times 10^{-2} \times \mathrm{Ra} - 2.88353 \times \varphi + 1.01835$	0.99630
	Glass balls	$1.0233 \times 10^{-2} \times \mathrm{Ra} - 1.73411 \times \varphi + 1.01366$	0.99667

Conclusion

Free convection inside a porous saturated rectangular cavity filled with Cu-water nanofluid was numerically studied. the study has revealed some important findings regarding the impact of *Ar*, the nanoparticles concentration, porosity and thermal conductivity of the porous media. The findings show that increasing the *Ar* leads to increase the flow stream inside the cavity. Moreover, adding more nanofluid particles deteriorate the heat enhancement. The main reason for the decline is primarily due to the increase in the dynamic viscosity caused by the existence of nanoparticles. In addition, as much as the thermal conductivity become considerable the effect of porosity is negligible. It is also observed that as the level of porosity in the porous material rises, there is typically a corresponding increase in the average Nusselt number. Furthermore, the highly conductive porous media can promote the flow regime. Additionally, an average Nusselt number correlation was found depending on Rayleigh number and φ. Lastly, results show that different flow structures may appear depending on the combination of values of *Ar*, ε, φ, and Rayleigh number

Nomenclature

Ar – aspect ratio
C_p – specific heat at a constant pressure, [$\mathrm{Jkg^{-1}K^{-1}}$]
g – acceleration of the gravity, [$\mathrm{ms^{-2}}$]
H – hight of the cavity, [m]
K – permeability, [$\mathrm{m^2}$]
k – thermal conductivity, [$\mathrm{Wm^{-1}K^{-1}}$]
L – width of the cavity, [m]
Nu – local Nusselt number
P – pressure, [Pa]
Ra – Rayleigh number of the porous medium
T – temperature, [K]
u,*v* – velocity components
V – velocity vector, [$\mathrm{ms^{-1}}$]
x,*y* – cartesian coordinates

Greek symbols

α – thermal diffusivity, [$\mathrm{m^2s^{-1}}$]
β – coefficient of thermal expansion, [$\mathrm{K^{-1}}$]
ε – porosity of the medium
θ – dimensionless temperature
μ – dynamic viscosity, [Pa·s]
ρ – density, [$\mathrm{kgm^{-3}}$]
φ – nanoparticles volume fraction
ψ – dimensionless velocity

Subscripts

avg – average quantity
f – fluid
mnf – nanofluid saturated with porous medium
m – clear fluid saturated with porous medium
nf – nanofluid
np – nanoparticle
p – particle
s – solid matrix of the porous medium

Superscript

~ – dimensional variable

References

[1] Nield, D. A., Bejan, A., *Convection in Porous Media*, Springer International Publishing, Cham, New York, USA, 2017
[2] Vafai, K., *Handbook of Porous Media*, CRC Press, Boca Raton, Fla., USA, 2005

[3] Chamkha, A. J., Al-Naser, H., Double-Diffusive Convection in an Inclined Porous Enclosure with Opposing Temperature and Concentration Gradients, *International Journal of Thermal Sciences, 40* (2001), 3, pp. 227-244
[4] Chamkha, A. J., Al-Naser, H., Hydromagnetic Double-Diffusive Convection in a Rectangular Enclosure with Uniform Side Heat and Mass Fluxes and Opposing Temperature and Concentration Gradients, *International Journal of Thermal Sciences, 41* (2002), 10, pp. 936-948
[5] Chamkha A. J., *et al.*, Mixed Convection Heat Transfer of Air inside a Square Vented Cavity with a Heated Horizontal Square Cylinder, *Numerical Heat Transfer, Part A: Applications, 59* (2011), 1, pp. 58-79
[6] Khanafer, K. M., Chamkha, A. J., Hydromagnetic Natural Convection from an Inclined Porous Square Enclosure with Heat Generation, *Numerical Heat Transfer, Part A: Applications, 33* (1998), 8, pp. 891-910
[7] Jung, S. Y., Park, H., Experimental Investigation of Heat Transfer of Al_2O_3 Nanofluid in a Microchannel Heat Sink, *International Journal of Heat and Mass Transfer, 179* (2021), 121729
[8] Sharifpur, M., *et al.*, Optimum Concentration of Nanofluids for Heat Transfer Enhancement Under Cavity Flow Natural Convection with TiO_2-Water, *International Communications in Heat and Mass Transfer, 98* (2018), Nov., pp. 297-303
[9] Anwar, M., *et al.*, Numerical Study for Heat Transfer Enhancement Using CuO Water Nanofluids Through Mini-Channel Heat Sinks for Microprocessor Cooling, *Thermal Science, 24* (2020), 5A, pp. 2965-2976
[10] Keblinski, P., *et al.*, Nanofluids for Thermal Transport, *Materials Today, 8* (2005), 6, pp. 36-44
[11] Asmadi, M. S., *et al.*, Nanoparticle Shape Effect on the Natural-Convection Heat Transfer of Hybrid Nanofluid Inside a U-shaped Enclosure, *Thermal Science, 26* (2022), 1B, pp. 463-475
[12] Rahimi, A., *et al.*, A Comprehensive Review on Natural Convection Flow and Heat Transfer: The Most Practical Geometries for Engineering Applications, *International Journal of Numerical Methods for Heat & Fluid Flow, 29* (2018), 3, pp. 834-877
[13] Sadeghi, M. S., *et al.*, On the Natural Convection of Nanofluids in Diverse Shapes of Enclosures: An Exhaustive Review, *Journal of Thermal Analysis and Calorimetry, 147* (2022), 1, pp. 1-22
[14] Izadi, S., *et al.*, A Comprehensive Review on Mixed Convection of Nanofluids in Various Shapes of Enclosures, *Powder Technology, 343* (2019), Feb., pp. 880-907
[15] Hashemi-Tilehnoee, M., *et al.*, Magnetohydrodynamic Natural Convection and Entropy Generation Analyses Inside a Nanofluid-Filled Incinerator-Shaped Porous Cavity with Wavy Heater Block, *Journal of Thermal Analysis and Calorimetry, 141* (2020), 5, pp. 2033-2045
[16] Xu, L., *et al.*, Numerical Investigating the Effect of Al_2O_3-Water Nanofluids on the Thermal Efficiency of Flat Plate Solar Collectors, *Energy Reports, 8* (2022), Nov., pp. 6530-6542
[17] Alklaibi, A. M., *et al.*, Experimental Investigation on the Performance of Hybrid Fe_3O_4 Coated MWCNT/Water Nanofluid as a Coolant of a Plate Heat Exchanger, *International Journal of Thermal Sciences, 171* (2022), 107249
[18] Yao, S., *et al.*, The Study of Natural Convection Heat Transfer of Nanofluids in a Partially Porous Cavity Based on Lattice Boltzmann Method, *Thermal Science, 23* (2019), 2B, pp. 1003-1015
[19] Dogonchi, A. S., *et al.*, A Numerical Investigation of Magnetohydrodynamic Natural Convection of Cu-Water Nanofluid in a Wavy Cavity Using CVFEM, *Journal of Thermal Analysis and Calorimetry, 135* (2019), 4, pp. 2599-2611
[20] Chamkha, A. J., *et al.*, Magnetohydrodynamic Nanofluid Natural Convection in a Cavity under Thermal Radiation and Shape Factor of Nanoparticles Impacts: A Numerical Study Using CVFEM, *Applied Sciences, 8* (2018), 12, 2396
[21] Alsabery, A. I., *et al.*, Mixed Convection of Al_2O_3-Water Nanofluid in a Double Lid-Driven Square Cavity with a Solid Inner Insert Using Buongiorno's Two-Phase Model, *International Journal of Heat and Mass Transfer, 119* (2018), Apr., pp. 939-961
[22] Belabid, J., *et al.*, Numerical Simulation for Impact of Copper/Water Nanofluid on Thermo-Convective Instabilities in a Horizontal Porous Annulus, *J. of Ther. Anal. and Calor., 138* (2019), 2, pp. 1515-1525
[23] Oztop, H. F., Abu-Nada, E., Numerical Study of Natural Convection in Partially Heated Rectangular Enclosures Filled with Nanofluids, *Int. Journal of Heat and Fluid Flow, 29* (2008), 5, pp. 1326-1336
[24] Redouane, F., *et al.*, Heat Flow Saturate of Ag/MgO-Water Hybrid Nanofluid in Heated Trigonal Enclosure with Rotate Cylindrical Cavity by using Galerkin Finite Element, *Scientific Reports, 12* (2022), 1, 2302
[25] Tiwari,R. K., Das, M. K., Heat Transfer Augmentation in a Two-Sided Lid-Driven Differentially Heated Square Cavity Utilizing Nanofluids, *Int. Journal of Heat and Mass Transfer, 50* (2007), 9, pp. 2002-2018

[26] Abu-Nada, E., Oztop, H. F., Effects of Inclination Angle on Natural Convection in Enclosures Filled with Cu-Water Nanofluid, *International Journal of Heat and Fluid Flow, 30* (2009), 4, pp. 669-678
[27] Haddad, Z., *et al*., A Review on Natural Convective Heat Transfer of Nanofluids, *Renewable and Sustainable Energy Reviews, 16* (2012), 7, pp. 5363-5378
[28] Sheremet, M. A., *et al*., Free Convection in a Square Cavity Filled with a Porous Medium Saturated by Nanofluid Using Tiwari and Das' Nanofluid Model, *Transport in Porous Media, 106* (2015), 3, pp. 595-610
[29] Bejan, A., On the Boundary Layer Regime in a Vertical Enclosure Filled with a Porous Medium, *Letters in Heat and Mass Transfer, 6* (1979), 2, pp. 93-102
[30] Gross, R. J., *et al*., The Application of Flux-Corrected Transport (fct) to High Rayleigh Number Natural Convection in a Porous Meduim, Begel House Inc., Danbury, Conn., USA, 1986
[31] Manole, D. M., Lage, J. L., Numerical Benchmark Results for Natural Convection in a Porous Medium Cavity, *Proceedings*, In Heat and Mass Transfer in Porous Media, ASME Conference 1992, Lakeland, Fla., USA, Vol. 216, pp. 55-60
[32] Baytas, A. C., Pop, I., Free Convection in Oblique Enclosures Filled with a Porous Medium, *International Journal of Heat and Mass Transfer, 42* (1999), 6, pp. 1047-1057
[33] Sun, Q., Pop, I., Free Convection in a Tilted Triangle Porous Cavity Filled with Cu-Water Nanofluid with Flush Mounted Heater on the Wall, *International Journal of Numerical Methods for Heat & Fluid Flow, 24* (2014), 1, pp, 2-20
[34] Sivasankaran, S., *et al*., Natural Convection in an Inclined Porous Triangular Enclosure with Various Thermal Boundary Conditions, *Thermal Science, 23* (2019), 2A, pp. 537-548
[35] Rao, P. S., Barman, P., Natural Convection in a Wavy Porous Cavity Subjected to a Partial Heat Source, *International Communications in Heat and Mass Transfer, 120* (2021), 105007
[36] Ghalambaz, M., *et al*., Free Convection in a Parallelogrammic Porous Cavity Filled with a Nanofluid Using Tiwari and Das' Nanofluid Model, *Plos One, 10* (2015), 5, e0126486

Paper submitted: April 5, 2023
Paper revised: July 12, 2023
Paper accepted: July 17, 2023